Desalination and Water Treatment
www.deswater.com

doi: 10.5004/dwt.2021.27469

231 (2021) 196–204
August

Preparation and characterization of blended membrane for copper removal application

Ali Bahader*, Sumaira Chan, Mohsin Nawaz, Fazal Suhrab Gul

Department of Chemistry, Hazara University Mansehra, Pakistan, Tel. +0092-997-414136; emails: alibahader@gmail.com (A. Bahader), sumairachan2015@gmail.com (S. Chan), mohsannawaz@hotmail.com (M. Nawaz), fsgulzai@gmail.com (F.S. Gul)

Received 6 January 2021; Accepted 28 May 2021

ABSTRACT

The current study elaborates the fabrication of the hydrophilic composite membrane (PVDF/PVP) for the removal of heavy metals present at low concentrations in water. The modified hydrophilic poly(vinylidene fluoride) (PVDF) composite membrane was prepared with a % ratio by blending hydrophilic poly(vinylpyrrolidone) (PVP) with hydrophobic PVDF. The Fourier transform infrared analysis reveals an interactive relationship between polymer and additives but fails to affect the crystal polymorphism of PVDF to an appreciable extent. Morphology of the fabricated composite membrane was inspected through scanning electron microscopy, revealing that PVP concentration strongly influences the overall morphology of the fabricated membrane. The low concentration of PVP produced macro-voids while the high concentration produced spongy and spherulitic morphology. Performance of the membrane was measured in terms of heavy metals removal, porosity, and water uptake. The results are suggestive of the fact that this membrane can be employed in real terms for the removal of heavy metals especially copper (Cu^{2+}) from water.

Keywords: Hydrophilic membrane; PVDF; PVP; Heavy metal

1. Introduction

Heavy metals are classified as hazardous materials since recognition of its dangerous impact on human life. They are potent carcinogens, due to its non-biodegradable nature and perseverance in the environment [1]. Among heavy metals, copper (Cu) is usually found at high concentrations in wastewater, owing to its use in different industries including metal finishing, ordinance factories, electroplating, and etching. The permissible level of copper (Cu) set by WHO and US EPA are 1.0 and 1.3 mg/L (ppm) in the aquatic environments, and this limit is often crossed, especially in developing countries, where strict regulations are not fully enforced [2]. Cu ingestion may cause acute and chronic medical conditions in humans such as hemolysis, irritation of the upper respiratory tract, gastrointestinal disturbance with vomiting and diarrhea, and a form of contact dermatitis. Therefore, it is necessary to have a proper check on Cu concentration in water [3,4].

Commonly, different types of adsorptive materials (activated carbon [5], natural materials like sawdust [6], graphene [7], and membrane [8], etc.) have been used for the removal of Cu from the water sample. These materials proved to efficiently remove copper from an aqueous solution. However, these adsorptive methods suffer from poor adsorption capacity due to its pH dependency/complex formation, laborious, low efficiency/cost ratio, and generation of sludge. The generated insoluble precipitates at pH < 6.0 of metal hydroxides restrict further adsorption of high metal ion concentration [5–8], which is cumbersome on an industrial scale. Therefore, such drawbacks necessitated having an adsorptive material, which scavenges metals or specifically copper (Cu) and regenerated after shedding the attached material and does not lose its

* Corresponding author.

capturing ability. In this scenario, polymer membrane is an ideal candidate, consuming less operational energy, simple, and easy to process with compactness in design [9]. It is estimated that nearly 53% of the total methods used in the purification of water are based on polymeric membranes. Material for the membrane is selected, keeping in view the stability of the porous structure, hydrophobicity/hydrophilicity balance, chemical resistivity, easy scalability, and mechanical strength. These parameters mostly affect the fouling (blockage of pores) of the membrane. Fouling is mainly caused by polarization of pores, hydrophobicity-hydrophilicity imbalance, thus leading to adsorption/deposition of particles/ions/organic matter, on the membrane surface [10]. Among different polymers poly(vinylidene fluoride) or PVDF is mostly used in wastewater treatment operations. PVDF a semicrystalline hydrophobic, chemical resistant polymer, and its various membranes/films can be produced through the non-solvent induced phase separation (NIPS) method. It is well known, that in NIPS crystallization of the component(s) in the non-solvent phase is triggered, leading to pores from nano- to micro-size scale [11].

To circumvent the problem of fouling and control over porosity, a variety of additives such as macromolecules [12], small organic materials (13), and inorganic salts [14] or particles [15] has also been tested.

Each additive has its own merits and demerits, but, the application area is water cleaning. Therefore, it is necessary to use a compound/polymer, which is biocompatible. Therefore, among such additives, the poly (vinylpyrrolidone) or PVP, is a suitable choice based on its non-toxicity, good miscibility, and hydrophilicity [16–18]. Similarly, it is reported that the addition of PVP may significantly change the surface properties/morphology of the membrane without macrovoids formation and impact on its filtration performance and porous structure [19]. But it must be remembered that PVDF also possesses the property of polymorphism, which was scarcely studied.

Therefore, in this work PVDF was modified with PVP (a well-known hydrophilic porogen), and its impact on the polymorphism and surface morphology of PVDF membrane, the removal efficiency was evaluated in the separation of copper (Cu) metal from water.

2. Experimental

2.1. Materials

Commercially available analytical grade chemicals were used during the entire experimental work. The chemicals were highly pure, so, further purification was not required and used as received. The (PVDF) pellet with mol. wt ~180,000 g/mol, PVP of average MW~Mw: 40,000 and N,N′–Dimethylformamide (DMF) were obtained from Sigma Aldrich, Germany.

2.2. Fabrication of membranes

The mixing ratio of the PVDF/PVP composite membrane is shown in Table 1. The appropriate amount of the dried PVDF and calculated mass of PVP was mixed in DMF. The mixture thus produced was stirred at 700°C for 4 h. The homogeneous mixture was cast into the already labeled clean Petri-dishes. The casted solution film was dipped into the water to separate the thin through non-solvent induced phase separation (NIPS) technique. The thin film was washed with enough water to clear the residual DMF followed by drying at 50°C as shown in Fig. 1. The films were characterized with Fourier transform infrared (FTIR) and scanning electron microscopy (SEM).

Table 1
Composition of samples used in this study (wt/wt%)

Sample code	PVP (wt%)	PVDF (wt%)
A	0	100
B	20	80
C	33	67
D	47	53

2.3. Characterization of fabricated membranes

To characterize the performance of the fabricated membrane, the following tests have been conducted.

2.3.1. Porosity

Membrane porosity was measured by the gravimetric method. Briefly, 2.5 cm in diameter of circular membrane sample was cut and soaked in glycerin. The porosity of membranes was estimated by Eq. (1):

$$\text{Porosity}(\%) = \frac{W_w - W_d}{A \cdot T \cdot \rho} \times 100 \quad (1)$$

where "A" is the surface area of the membrane in m^2, "T" is the membrane's thickness in cm and "ρ" is the density of the wetted liquid in (g/cm^3), W_w is the weight of the wetted membrane sample, and W_d is the weight of dry membrane sample.

2.3.2. Water uptake

Uptake of water by different samples (membranes) were calculated gravimetrically, a circular (2.5 cm in diameter) membrane sample was cut and weighed/designated as W_0 for the dry sample. W_f is the uptake of water by membrane samples which is calculated by wetting and shaking sample with swelling liquid (water) in a beaker for 12 h at ambient temperature. The % uptake of water was estimated from Eq. (2) and taken as hydrophilic property:

$$W_{\text{uptake}} = \frac{W_f - W_0}{W_0} \times 100 \quad (2)$$

2.3.3. Separation efficiency of membrane

1 M $CuSO_4$ designated as solution 1 was prepared and then standardized against 2 M $Na_2S_2O_7$ designated

solution 2. The $CuSO_4$ solution is then passed through each sample membrane and the filtrate from each sample was titrated against solution 2 again, and the amount of Cu present in the filtrate was calculated by using Eq. (3):

$$M_1V_1 = M_2V_2 \tag{3}$$

where M_1 and V_1 are the molarity and volume of solution No. 1 ($CuSO_4$), while M_2 and V_2 are the molarity and volume of solution No. 2 ($Na_2S_2O_7$) consumed during the titration experiment. From the molar calculation, the amount of Cu was calculated in the filtrate.

The metal removes by the prepared membrane was calculated using Eq. (4):

$$\%\ \text{Removal} = \left(1 - \frac{C_p}{C_f}\right) \times 100 \tag{4}$$

where C_p is the concentration of filtrate and C_f is the concentration of feed solution.

3. Results and discussion

3.1. Surface topology of the membranes

All membranes show the asymmetric morphology characterized by the rough and bubbly domain (often labeled as spherulite domain). The surface morphology of the blended membrane was visualized through SEM bearing no. JSM-IT-100, JEOL, Japan. The neat PVDF membrane is distinguished by the presence of a dominant spherulite phase with a rough surface. Fig. 2 represents the morphological characteristics of the as-prepared pristine PVDF membrane. Generally, the fabricated PVDF exhibits three crystalline phases of α, β, and γ phases, and intrinsically different from one another in terms of chain orientation and polarity originated from re-arrangement of the fluorinated skeleton [20]. This factor might be taken into consideration for the generation of pores, as similar phases tend to accumulate forming a separate domain leaving behind empty space called voids/pores.

The polar phase tends to retain a small fraction of water, which directs itself away from the non-polar α phase of PVDF. This incompatibility at the molecular level generates an uneven/rough surface that gives rise to support to the already narrated assumption. In the inset of Fig. 3, small pores were identified through ImageJ software.

Similarly, in Fig. 3, the channelized finger-like structure with voids can be seen. The voids seem to generate from the knitting (attraction/repulsion) of entangled polymer chains. The morphology of the pores is irregular and present a network structure. Another important observation, which can be noted is the creation of mixed pores (large/small). It means pores are generated through competitive processes of de-mixing (attraction/repulsion) of solvent in the coagulant and polymer dope. The presence of PVP being surfactant/amorphous may attenuate the thermodynamic stability of the crystallized film, which favors competitive de-mixing processes and generate macro-voids [21–25].

It was observed physically that this membrane is more flexible as compared to other membranes. It is also suggestive of the fact that an attenuated solid-air interface exists in the membrane, which gives toughness to the material through the polymer-air interface. According to Table 2, the addition of amorphous PVP into the PVDF matrix leads to a more porous structure with increased porosity. With further increase in the concentration of amorphous PVP, the surface of the film changes to spongy nature, with the existence of numerous small pores as can be seen in Fig. 4C1 and C2.

When the amount of PVP is increased as indicated in Fig. 5D1 and D2, a very different structure can be seen. The surface is full of spherulitic structures, but pores are generated inside this structure. The possible explanation may be the spherulites during the formation stage engulf a small fraction of the PVP, which is leach out in the coagulation bath due to its solubility in the water and thus produced small pores. The burst-out structure may be formed by escaping/leaching of PVP into the water coagulation bath or any other impurities at the time of crystallization of PVDF.

3.2. Crystal polymorphism and chain interaction

For investigating functional groups interactions between the ingredients of the nanocomposites FTIR study of neat and different blended membranes were conducted in 1,000–400 cm^{-1} (Fig. 6), and in 2,000–1,000 cm^{-1} range (Fig. 7) for easy readability. Calibration of the instrument was done with styrene as a standard before the characterization of the thin-film sample.

In Figs. 6 and 7A, the pristine PVDF generated peaks at position 410; 489; 510; 532; 613; 763; 795; 841; 855; 873; 976; 1,065; 1,182; 1,274; 3,025 and 3,372 cm^{-1}. According to literature the signals 410, 532, 613, 763, 855, and 976 cm^{-1} were assigned to the presence of non-polar α form. The

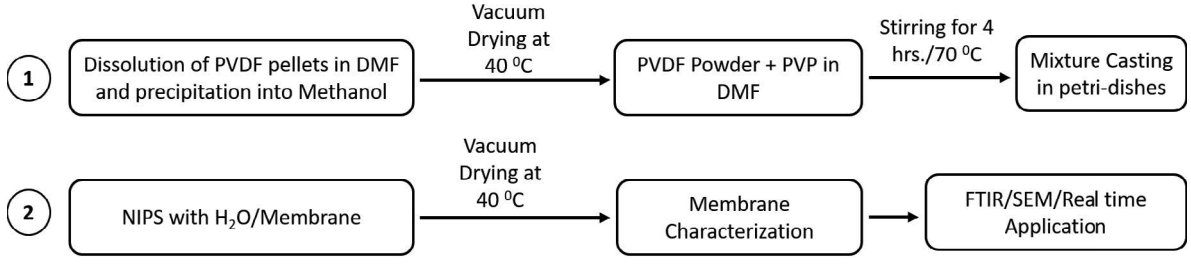

Fig. 1. Schematic diagram for preparation of membranes.

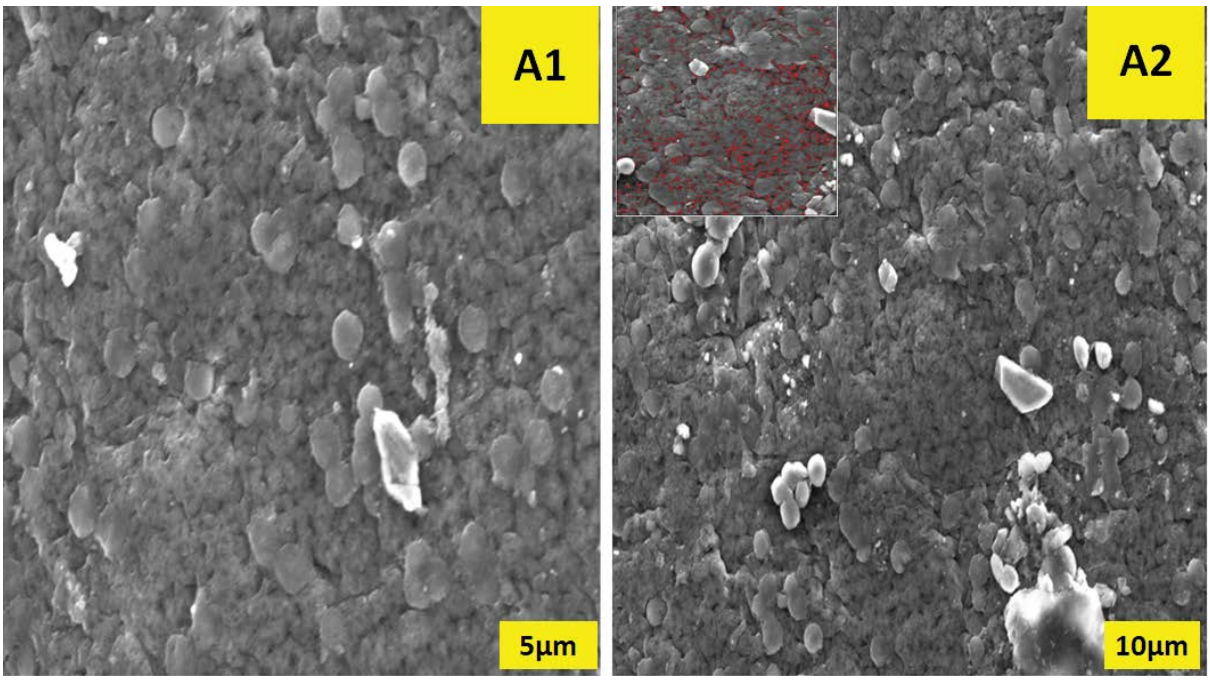

Fig. 2. Micrographs of the sample (A) at a magnification of A1 = 5 µm, A2 = 10 µm.

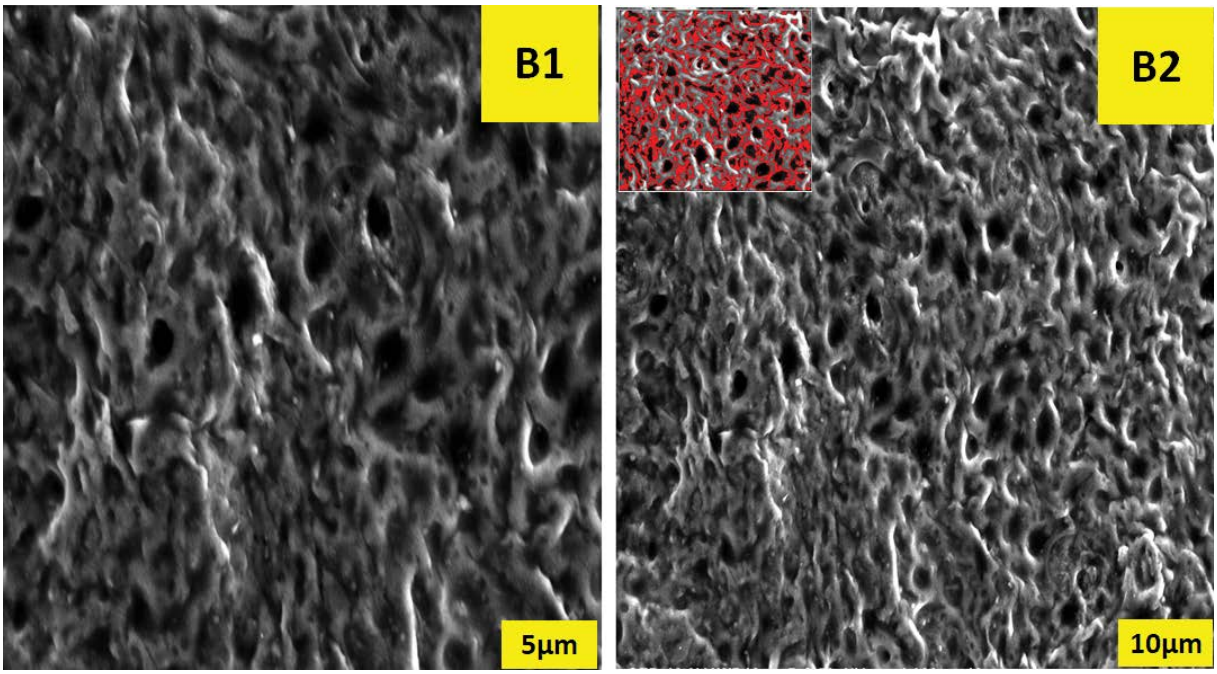

Fig. 3. SEM micrographs of the sample (B) at a magnification of B1 = 5 µm, B2 = 10 µm.

β phase contribution was confirmed from the presence of 510; 840 and 1,274 cm^{-1} peaks [13, 20]. These bending and wagging vibrations reveals the existence of CF_2 group in different orientations, on which PVDF is classified as α and β phases.

The α phase is the stable one while β phase is unstable and requires special treatment or insertion of the polar molecule into the macromolecular galleries to stabilize it. It is well-established that the absorption peak due to polar β-phase appears around 839/840 cm^{-1} and is characterized by a mixed mode of CF_2/CH_2 stretching vibrations seen in sample A as highlighted in Figs. 6 and 7. It is possible that polar DMF was used and might be responsible for mixed polar phases (α and β) generation, as present in the spectrum of pure PVDF. Moreover, it is well-established that FTIR spectra of PVP demonstrate a strong absorption

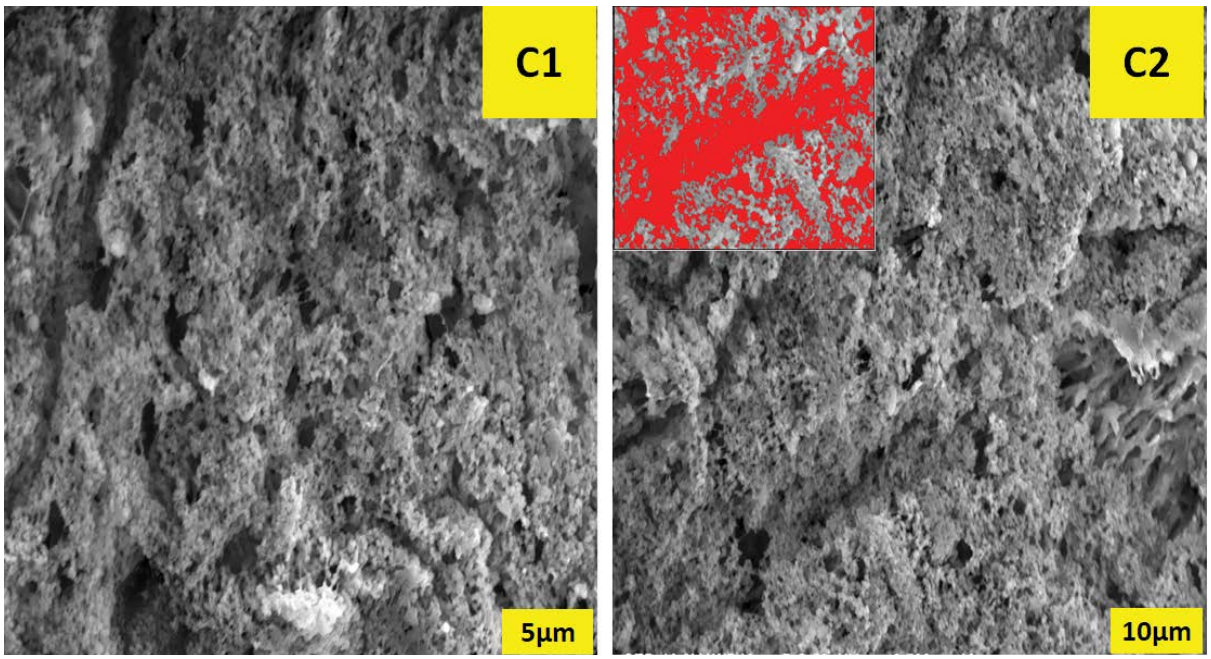

Fig. 4. SEM micrographs of the sample (C) at a magnification of C1 = 5 µm, C2 = 10 µm.

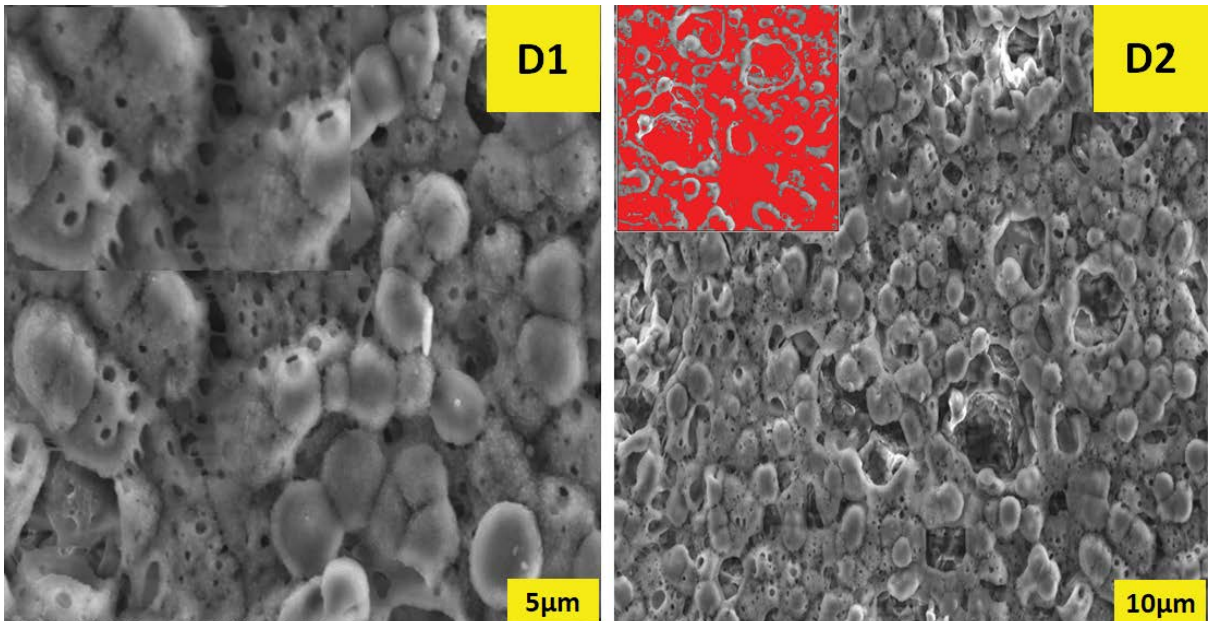

Fig. 5. SEM micrographs of (D) at a magnification of D1 = 5 µm, D2 = 10 µm.

Table 2
Statistical data of the pore size, % porosity, % water uptake and % removal of PVDF/PVP composite membranes

S. No.	Sample code	Pore size (µm)	% Water uptake	% removal	% porosity
1	A	0.101	39.78	30	5.83
2	B	4.757	50.07	39	29.96
3	C	0.246	60.02	50	54.67
4	D	0.143	81.07	62	65.14

peak at 1,600 cm^{-1} due to C=O in the PVP skeleton [17]. The PVP also shows asymmetric CH_2 stretching vibrations in the region around 2,900 cm^{-1}. The bands at 1,423 and 1,371 cm^{-1} also correspond to the CH de-formation modes from the CH_2 present in the PVP ring as shown in Figs. 6 and 7B. Therefore, these regions may be taken as an indication for the development of the interactions between the PVDF and PVP as described elsewhere [16].

In Figs. 6 and 7B, where 20 wt% of PVP was added into the dope solution of the PVDF, the following peaks were recorded, which are centered at 420; 485; 510; 532; 613; 762; 796; 840; 874; 1,039; 1,109; 1,181; 1,404; 1,652; 2,884; 2,942 and 3,319 cm^{-1}. It can be seen from the data that some signal seen in the case of original PVDF appears again at 510, 532, and 613 cm^{-1}, which confirms that some fraction of the α phase is still present [20]. The new peaks also appear by a one-degree shift to lower/higher value showing the development of specific interactions between PVP and PVDF. The PVP shows strong absorption at 1,600 cm^{-1} but here it appears at 1,652 cm^{-1} shows the shift in its position. This is also a strong indication for the development of interaction between the acidic hydrogen of the PVDF and electronegative oxygen and nitrogen of PVP [16].

Figs. 6 and 7C show the FT-IR spectra of the sample (C) having 33 wt% PVP. The signal observed were 412; 489; 532; 614; 762; 796; 841; 854; 874; 976; 1,066; 1,182; 1,382; 1,404; 1,669; 3,025 and 3,378 cm^{-1}. The spectra clearly show that peaks are shifted from their earlier position and appear at 1,669 cm^{-1} while at the same time some new peaks (3,025 and 3,378 cm^{-1}) appear. This shows that interactions become stronger due to the increase in the amount of PVP, and the band appears at higher values. The peaks at 3,025 and 3,378 cm^{-1} might be suggested of the fact that the existence of polar fraction (β/γ) in the subject material may retain a small amount of the strongly polar H_2O molecules, which mostly appear in this region due to the possible existence of polarized fraction.

Figs. 6 and 7D are the FTIR spectra of the sample having 47 wt% of PVP. The peaks recorded were visualized at 418; 480; 510; 839; 878; 1,073; 1,171; 1,233; 1,272; 1,404; 1,463; 1,496; 1,662 and 3,395 cm^{-1}. This also shows that PVP being miscible with PVDF and able to play role in the structural polymorphism of crystallized PVDF. It is reported that the band at 875 cm^{-1} sifted to 876/877 cm^{-1} shows the interaction between CF_2 and C=O of the PVP ring [26].

4. Performance of fabricated membranes

4.1. Water uptake

Water uptake studies show good evidence to support the hydrophilic nature of the membranes. The % water uptake of samples A, B, C, and D are 39.78%, 50.07%, 60.02%, and 81.07%, respectively, as shown in Table 2, which clearly shows that the PVDF-PVP blended membrane is transformed from hydrophobic to hydrophilic with the addition of PVP. It is well-established fact, that PVDF is hydrophobic but due to a small fraction of the β phase it can retain water as confirmed from the FTIR signals. The data confirmed that the addition of PVP leads to the generation of polar fraction, which selectively permits water molecule through the phenomenon of pores polarization, and responsible for the increasing trend depicted in Fig. 8.

By increasing PVP concentration in the dope solution, the hydrophilic sites are also increasing and may engulf some aqueous fraction through H-bonding forming a fine film that boosts the water transportation through membranes, which prevents hydrophobic foulants to adhere to the surface of the membrane [18,27].

4.2. Porosity (%)

Interaction of hydrophilic PVP with the hydrophobic PVDF may be responsible for the development of spongy structure as observed in SEM analysis and conclusively suggesting the presence of network structure. Consequently, by increasing the concentration of PVP in the casting solution the porosity of the membrane is enhanced. According to Table 2, the % porosity of samples A, B, C, and D, are

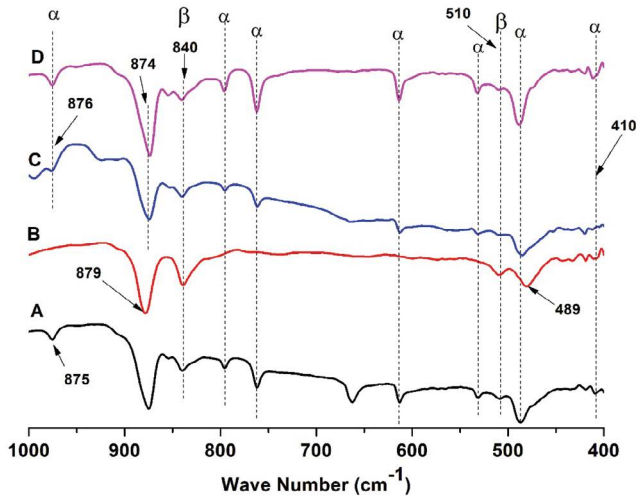

Fig. 6. Comparative FTIR spectra for samples (A–D) in the range 400–1,000 cm^{-1}.

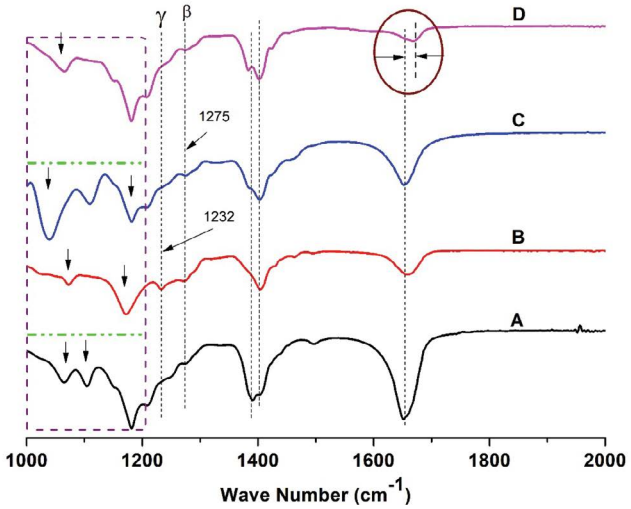

Fig. 7. Comparative FTIR spectra for samples (A–D) in the range 1,000–2,000 cm^{-1}.

5.838%, 29.961%, 54.677%, 65.147%, respectively. In general, porosity is the measure of the void fraction, that is, the membrane having finger-like structure and macro void fraction with respect to the spongiform membrane, confirmed by SEM analysis and visualized in Fig. 9.

It is clear from the data linked to sample B, C, and D that increment in PVP concentration reduces the pore size and increase its number per unit area through molecular interactions (attraction/repulsion) [28]. It may be due to the competitive demixing of the solvents in the dope and casting solution. It is believed that PVP increases the viscosity of the solution, and when this dense solution is poured into the casting solvent (H_2O), the PVDF solvating medium (DMF) tends to migrate from the nascent film into the water and aids in PVDF crystallization. On the contrary, the amorphous nature of PVP may contribute toward the delayed crystallization of PVDF.

4.3. Separation efficiency

The prepared membranes were utilized for the removal of heavy metals especially copper (Cu) as graphically shown in Fig. 10.

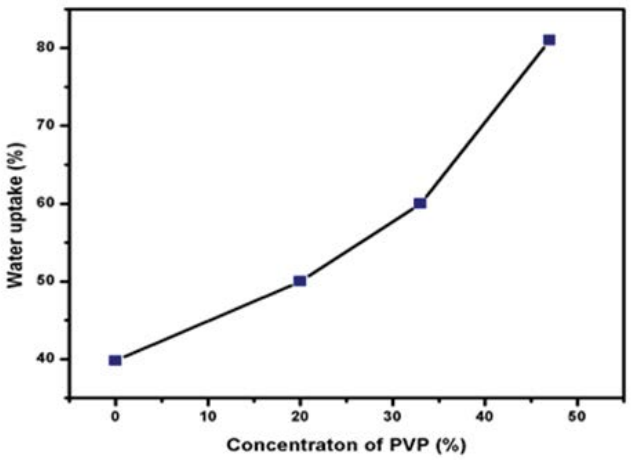

Fig. 8. Water uptake by membranes (%).

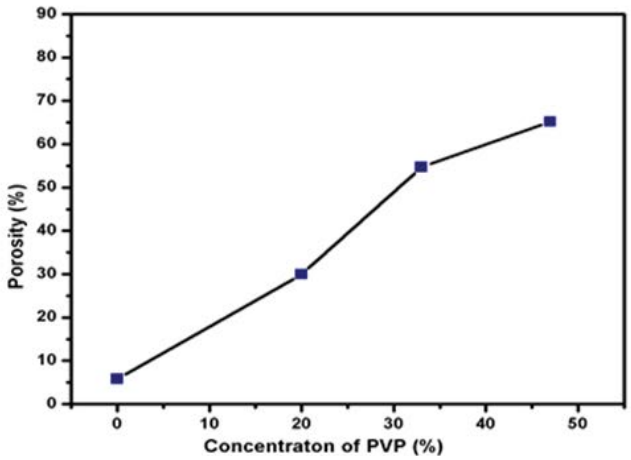

Fig. 9. Porosity (%) of membranes.

The % removal data for the sample A, B, C, and D are as follows 30%, 39%, 50%, and 62%, respectively. Results show that the removal efficiency of copper by blended membranes were increased with the increase in PVP concentration in the polymer dope solutions. Such an increase leads to the production of more porous membranes with small pore size.

In Fig. 11, the studied parameters are collectively displayed graphically, showing direct relation of porosity with water uptake and copper removal efficiency of the different blended membrane(s).

The probable explanation for this might be the establishment of interactive forces between the electronegative fluorine atom and the positive charge center present in the PVP ring. Such charge equilibration may leave an appreciable negative charge for the scavenging of metal ions by the membrane surface and appear in increase % removal [29].

4.4. Mechanism of high separation efficiency of membrane

The PVP a well-known hydrophilic additive while PVDF is hydrophobic, but both are miscible. When such

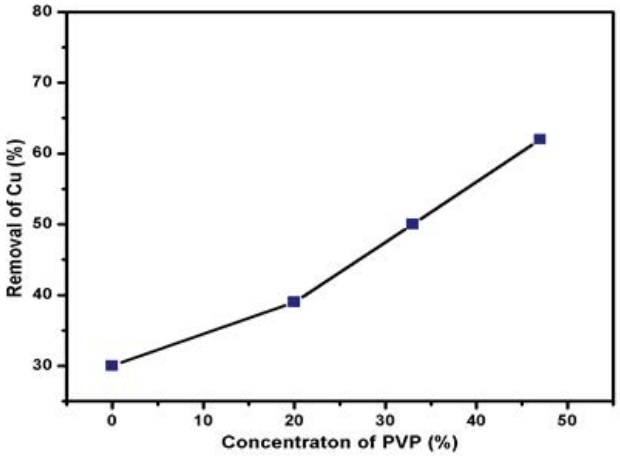

Fig. 10. Removal of Cu (%) from composite membranes.

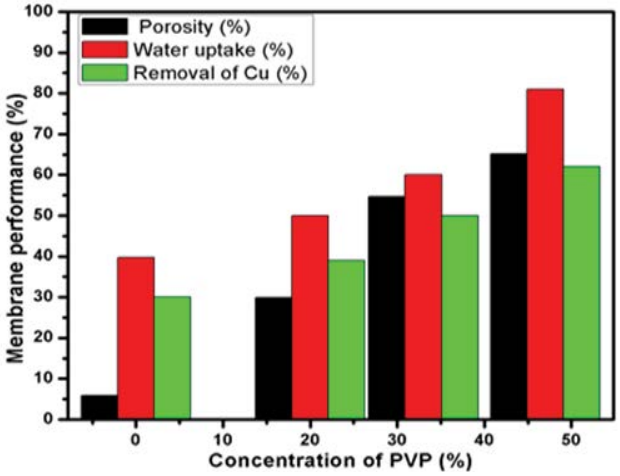

Fig. 11. Comparison of membrane performance.

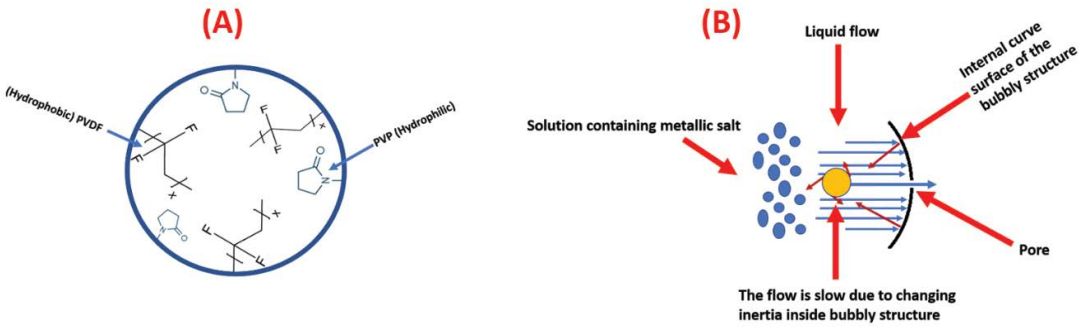

Fig. 12. The proposed (A) cross-sectional view of membrane's pores (B) mechanistic view for high separation efficiency.

blend is exposed to the aqueous environment, the PVP may absorb water molecules and tends to swell, while at the same instant PVDF try to stretch away from it. This stretching or de-mixing phenomenon creates pores and a bubbly structure as seen in Fig. 5. This process may occur inside a bubbly structure and create small pores. It is well-established fact that liquid when flowing in a circular path, changes its direction resulting in the sluggishness of velocity, which gives an opportunity for the copper sulfate crystal to crystallize at that moment. Once the nuclei formed, facilitates heterogeneous nucleation, and result into the narrowing of the pores due to the deposition of copper sulfate crystals. It may also probable that the increased concentration of PVP leads to swelling and gelation, which is reported to enhance the crystallization of the entrapped molecule [30]. Such behavior may increase the removal percentage of copper according to the mechanism proposed in Fig. 12.

5. Conclusions

Hydrophobic PVDF membrane was modified via phase inversion method using different concentrations of hydrophilic PVP. The blending of PVDF with PVP leads to produce a more porous structure with mixed pore morphology. The morphology of the fabricated membrane is strongly influenced by the concentration of PVP in the polymeric dope solution. With low contents of PVP, the membrane with large voids is obtained but with increasing content of PVP, the wide pore structure transforms into a smaller one through de-mixing of the interfaces involved and developed interactions among the ingredients. The morphology is asymmetric and strongly influences the % removal of heavy metal, water uptake, and porosity. The increase in the water uptake is convincing proof of the hydrophilic modification of the fabricated PVDF membranes. Overall, PVP a well-known hydrophilic additive succeeded in pore formation and upgraded the performance of the blended membrane. The outcomes of this work revealed that modified membranes have enhanced hydrophilicity, asymmetric porous structure, and effective in the removal of copper ions from water.

References

[1] Z. Fu, S. Xi, The effects of heavy metals on human metabolism, Toxicol. Mech. Methods, 30 (2020) 167–176.
[2] M. Kumar, A. Puri, A review of permissible limits of drinking water, Indian J. Occup. Environ. Med., 16 (2012) 40–44.
[3] S. Chowdhury, M.A.J. Mazumder, O.A. Attas, T. Husain, Heavy metals in drinking water: occurrences, implications, and future needs in developing countries. Sci. Total Environ., 569 (2016) 476–488.
[4] H. Demiral, C. Güngör, Adsorption of copper(II) from aqueous solutions on activated carbon prepared from grape bagasse, J. Cleaner Prod., 124 (2016) 103–113.
[5] M. Karnib, A. Kabbani, H. Holail, Z. Olama, Heavy metals removal using activated carbon, silica and silica activated carbon composite, Energy Procedia, 50 (2014) 113–120.
[6] B. Yu, Y. Zhang, A.S. Shukla, S. Shyam, K.L. Dorris, The removal of heavy metal from aqueous solutions by sawdust adsorption — removal of copper, J. Hazard. Mater., 80 (2000) 33–42.
[7] W. Wu, Y. Yang, H. Zhou, T. Ye, Z. Huang, R. Liu, Y. Kuang, Highly efficient removal of Cu(II) from aqueous solution by using graphene oxide, Water Air Soil Pollut., 224 (2013) 1372 (1–8), doi: 10.1007/s11270-012-1372-5.
[8] K.C. Khulbe, T. Matsuura, Removal of heavy metals and pollutants by membrane adsorption techniques, Appl. Water Sci., 8 (2018) 19 (1–30), doi: 10.1007/s13201-018-0661-6.
[9] B.A. Rashdi, Heavy metals removal using adsorption and nanofiltration techniques, Sep. Purif. Rev., 40 (2011) 209–259.
[10] Z. Cao, Microscopic mechanism of membrane fouling in microfiltration, Desal. Water Treat., 57 (2015) 6652–6657.
[11] J.T. Jung, J.F. Kim, H.H. Wang, E.D. Nicolo, E. Drioli, Y.M. Lee, Understanding the non-solvent induced phase separation (NIPS) effect during the fabrication of microporous PVDF membranes via thermally induced phase separation (TIPS), J. Membr. Sci., 514 (2016) 250–263.
[12] P. Sakellariou, R.C. Rowe, E.F.T. White, A study of the leaching/retention of water-soluble polymers in blends with ethylcellulose using torsional braid analysis, J. Controlled Release, 7 (1988) 147–157.
[13] C. Xing, M. Zhao, L. Zhao, J. You, X. Cao, Y. Li, Ionic liquid modified poly(vinylidene fluoride): crystalline structures, miscibility, and physical properties, Polym. Chem., 4 (2013) 5726–5734.
[14] R. Bodmeier, O. Paeratakul, leaching of water-soluble plasticizers from polymeric films prepared from aqueous colloidal polymer dispersions, Drug Dev. Ind. Pharm., 18 (1992) 1865–1882.
[15] M. Safarpour, A. Khataee, V. Vatanpour, Preparation of a novel polyvinylidene fluoride (PVDF) ultrafiltration membrane modified with reduced graphene oxide/titanium dioxide (TiO_2) nanocomposite with enhanced hydrophilicity and antifouling properties, Ind. Eng. Chem. Res., 53 (2014) 13370–13382.
[16] N. Chen, L. Hong, Surface phase morphology and composition of the casting films of PVDF–PVP blend, Polymer, 43 (2002) 429–1436.
[17] I.A. Safo, M. Werheid, C. Dosche, M. Oezaslan, The role of polyvinylpyrrolidone (PVP) as a capping and structure-directing agent in the formation of Pt nanocubes, Nano Adv., 1 (2019) 3095–3106.
[18] M. Nasir, H. Matsumoto, M. Minagawa, A. Tanioka, T. Danno, H. Horibe, Preparation of porous PVDF nanofiber from PVDF/

PVP blend by electrospray deposition, Polym. J., 39 (2007) 1060–1064.
[19] C. Hying, E. Staude, The influence of polyvinylpyrrolidone (PVP) in polyetherimid/PVP blend membranes upon vapor separation, J. Membr. Sci., 144 (1998) 251–257.
[20] C. Xing, L. Zhao, J. You, W. Dong, X. Cao, Y. Li, Impact of ionic liquid-modified multiwalled carbon nanotubes on the crystallization behavior of poly(vinylidene fluoride), J. Phys. Chem. B, 116 (2012) 8312–8320.
[21] J.J. Qin, Y.M. Cao, L.S. Lee, Development of a LCST membrane forming system for cellulose acetate ultrafiltration hollow fiber, Sep. Purif. Technol., 42 (2005) 291–295.
[22] I.C. Kim, K.H. Lee, Effect of poly (ethylene glycol) 200 on the formation of a polyetherimide asymmetric membrane and its performance in aqueous solvent mixture permeation, J. Membr. Sci., 230 (2004) 183–188.
[23] Q.Z. Zheng, Y.N. Yang, Rheological and thermodynamic variation in polysulfone solution by PEG introduction and its effect on kinetics of membrane formation via phase-inversion process, J. Membr. Sci., 279 (2006) 230–237.
[24] Q.Z. Zheng, P. Wang, Y.N. Yang, D.J. Cui, The relationship between porosity and kinetics parameter of membrane formation in PSF ultrafiltration membrane, J. Membr. Sci., 286 (2006) 7–11.
[25] H.J. Kim, R.K. Tyagi, A.E. Fonda, K. Jonasson, The kinetic study for asymmetric membrane formation via phase-inversion process, J. Appl. Polym. Sci., 62 (1996) 621–629.
[26] S. Manna, A.K. Nandi, Piezoelectric β polymorph in poly(vinylidene fluoride)-functionalized multiwalled carbon nanotube nanocomposite films, J. Phys. Chem. C, 111 (2007) 14670–14680.
[27] S.K. Ghosh, W. Rahman, T.R. Middya, S. Sen, D. Mandal, Improved breakdown strength and electrical energy storage performance of gamma-poly(vinylidene fluoride)/unmodified montmorillonite clay nano-dielectrics, Nanotechnology, 27 (2016) 215401–09, doi: 10.1088/0957-4484/27/21/215401.
[28] W.Z. Lang, Y.J. Guo, L.F. Chu, Evolution of the precipitation kinetics, morphologies, permeation performances, and crystallization behaviors of polyvinylidene fluoride (PVDF) hollow fiber membrane by adding different molecular weight polyvinylpyrrolidone (PVP), Polym. Adv. Technol., 22 (2011) 1720–1730.
[29] P. Martins, A.C. Lopes, S.L. Mendez, Electroactive phases of poly (vinylidene fluoride): determination, processing and applications, Prog. Polym. Sci., 39 (2014) 683–706.
[30] Y. Diao, K.E. Whaley, M.E. Helgeson, M.A. Woldeyes, P.S. Doyle, A.S. Myerson, T.A. Hatton, B.L. Trout, Gel-induced selective crystallization of polymorphs, J. Am. Chem. Soc., 134 (2012) 673–684.